



ELSEVIER

Available online at www.sciencedirect.com

SCIENCE @ DIRECT®

Physica A 335 (2004) 455–486

PHYSICA A

www.elsevier.com/locate/physa

Recursive graphical solution of closed Schwinger–Dyson equations in ϕ^4 -theory. (I). Generation of connected and one-particle irreducible Feynman diagrams

Axel Pelster*, Konstantin Glaum

Institut für Theoretische Physik, Freie Universität Berlin, Arnimallee 14, Berlin 14195, Germany

Received 29 September 2003; received in revised form 8 December 2003

Abstract

Using functional derivatives with respect to the free correlation function we derive a closed set of Schwinger–Dyson equations in ϕ^4 -theory. Its conversion to graphical recursion relations allows us to systematically generate all connected and one-particle irreducible Feynman diagrams for the two- and four-point function together with their weights.

© 2003 Elsevier B.V. All rights reserved.

1. Introduction

Many quantities observed in modern particle or statistical physics are modified due to fluctuation corrections. The corresponding theoretical computations are usually quite lengthy, which makes their automation mandatory. The current status of the automatic calculation of Feynman diagrams is reviewed in Refs. [1–3]. There, the most important theoretical techniques are introduced and their usefulness is demonstrated with the help of simple examples. In addition, a survey over frequently used programs and packages is provided, discussing their abilities and fields of applications.

The first step towards an automatic calculation of Feynman diagrams is their construction and the determination of their weights in different field theories. For this purpose various convenient computer programs have been designed as, for instance, FEYNARTS [4,5], QGRAF [6], or DIANA [7]. Some of them are based on a combinatorial enumeration of all possible ways of connecting vertices by lines according to

* Corresponding author.

E-mail addresses: pelster@physik.fu-berlin.de (A. Pelster), glaum@physik.fu-berlin.de (K. Glaum).

Feynman's rules. Others use a systematic generation of homeomorphically irreducible star graphs [8,9]. The latter approach is quite efficient and popular at higher orders. It has, however, the conceptual disadvantage that it renders, at an intermediate stage, numerous superfluous diagrams with different vertex degrees, which have to be discarded at the end. Further promising methods have been proposed in Refs. [10,11]. Whereas the first one is based on a bootstrap equation that uses only the free-field value of the energy as an input, the second one combines Schwinger–Dyson equations with the two-particle irreducible (“skeleton”) expansion.

A well-established method to obtain perturbation expressions in field theory relies on the source concept of Julian Schwinger [12]. To this end, one introduces in the given energy functional local external currents, which are linearly coupled to the fields (see, for instance, the textbooks [13–25]). This makes the corresponding partition function a generating functional, which allows one to calculate all n -point functions from functional derivatives with respect to these external currents. Another more sophisticated and not well-known approach uses artificial tensorial currents, so the n -point functions follow from a smaller number of functional derivatives. This technique has influenced the development of many-body theory for a long time [26–31]. More contemporary applications of these functional analytic methods were developed for quantum and statistical field theory in Refs. [32–34]. They aimed at systematically constructing certain classes of Feynman diagrams of a field theory together with their weights by graphically solving a closed set of functional differential equations. Furthermore, they developed nonperturbative approximations by successively eliminating corrections to the lines and vertices with the help of higher Legendre transformations.

Recently, we have elaborated a related program, which abandons the introduction of artificial tensorial currents. Instead, we consider the Feynman diagrams of a field theory as functionals of their graphical elements, i.e., their lines and vertices. Functional derivatives with respect to these graphical elements are represented by removing lines or vertices of a Feynman diagram in all possible ways. Our program is then based on the observation that the knowledge of the vacuum energy implies the knowledge of the entire theory (“The vacuum is the world”) [12,35], and proceeds in the following four steps. First, a nonlinear functional differential equation for the free energy is derived as a consequence of the field equations. Subsequently, this functional differential equation is converted into a recursion relation for the respective perturbative expansion coefficients of the free energy. From its graphical solution, the connected vacuum diagrams are constructed together with their weights. Finally, all diagrams of n -point functions are obtained by removing lines or vertices from the connected vacuum diagrams. This program has been recently used to systematically generate all Feynman diagrams of ϕ^4 -theory of second-order phase transitions in the disordered, symmetric phase [36] and in the ordered, broken-symmetry phase [37,38]. In the same way we have treated Ginzburg–Landau theory [39], quantum electrodynamics [40], and many-body theory [41].

Furthermore, we have developed a modification of this program, which does not start from the vacuum diagrams. Instead, it aims at directly generating the Feynman diagrams of n -point functions, which obey an infinite hierarchy of Schwinger–Dyson equations [13–25]. Using functional derivatives with respect to the free correlation

functions and the vertices has allowed us to close these Schwinger–Dyson equations in a functional analytic sense. They can be turned into graphical recursion relations for the Feynman diagrams of the respective connected and one-particle irreducible n -point functions. From these, the corresponding vacuum diagrams follow by short-circuiting external legs. So far, this functional closure of the Schwinger–Dyson equations has been performed for quantum electrodynamics [42].

The purpose of the present paper is to apply this functional–analytic approach to the ϕ^4 -theory of second-order phase transitions in the disordered, symmetric phase. A short outline of this program was already published in Ref. [43]. To this end we derive in Section 2 a closed set of equations for the connected two- and four-point function. Analogously, we determine in Section 3 a closed set of Schwinger–Dyson equations for the self-energy and the one-particle irreducible four-point function. In both cases, the closed set of Schwinger–Dyson equations can be converted into graphical recursion relations for the corresponding connected and one-particle irreducible Feynman diagrams in ϕ^4 -theory. From these the respective connected vacuum diagrams follow by short-circuiting external legs.

2. Scalar ϕ^4 -theory

Euclidean ϕ^4 -theories in d dimensions are useful models for a large family of universality classes of continuous phase transitions [25]. In particular, the $O(N)$ -symmetric ϕ^4 -theory serves to describe the critical phenomena in dilute polymer solutions ($N=0$), Ising- and Heisenberg-like magnets ($N = 1, 3$), and superfluids ($N = 2$). In all these systems, the thermal fluctuations of a self-interacting scalar order parameter field ϕ with N components are controlled by the Ginzburg–Landau energy functional

$$E[\phi] = \int d^d x \left\{ \frac{1}{2} \sum_{\alpha=1}^N \phi_{\alpha}(x)(-\partial_x^2 + m^2)\phi_{\alpha}(x) + \frac{g}{24} \left[\sum_{\alpha=1}^N \phi_{\alpha}^2(x) \right]^2 \right\}, \tag{1}$$

where the mass m^2 is proportional to the temperature deviation from the critical point and g denotes the coupling constant. In the following it turns out to be advantageous to rewrite the Ginzburg–Landau energy functional (1) as

$$E[\phi] = \frac{1}{2} \int_{12} G_{12}^{-1} \phi_1 \phi_2 + \frac{1}{24} \int_{1234} V_{1234} \phi_1 \phi_2 \phi_3 \phi_4. \tag{2}$$

In this short-hand notation, the spatial and tensorial arguments of the order parameter field ϕ , the bilocal kernel G^{-1} , and the quartic interaction V are indicated by simple number indices, i.e.,

$$1 \equiv \{x_1, \alpha_1\}, \quad \int_1 \equiv \sum_{\alpha_1=1}^N \int d^d x_1, \quad \phi_1 \equiv \phi_{\alpha_1}(x_1). \tag{3}$$

The kernel G^{-1} represents the functional matrix

$$G_{12}^{-1} \equiv G_{\alpha_1, \alpha_2}^{-1}(x_1, x_2) = \delta_{\alpha_1, \alpha_2}(-\partial_{x_1}^2 + m^2)\delta(x_1 - x_2), \tag{4}$$

while the interaction V is given by the functional tensor

$$\begin{aligned}
 V_{1234} &\equiv V_{\alpha_1, \alpha_2, \alpha_3, \alpha_4}(x_1, x_2, x_3, x_4) \\
 &= \frac{g}{3} (\delta_{\alpha_1, \alpha_2} \delta_{\alpha_3, \alpha_4} + \delta_{\alpha_1, \alpha_3} \delta_{\alpha_2, \alpha_4} + \delta_{\alpha_1, \alpha_4} \delta_{\alpha_2, \alpha_3}) \delta(x_1 - x_2) \delta(x_1 - x_3) \delta(x_1 - x_4),
 \end{aligned}
 \tag{5}$$

both being symmetric in their indices. For the purpose of this paper we shall leave the kernel G^{-1} in the energy functional (2) completely general, except for the symmetry with respect to its indices. By doing so, we regard the energy functional (2) as a functional of the kernel G^{-1} :

$$E[\phi] = E[\phi, G^{-1}].
 \tag{6}$$

As a consequence, all global and local statistical quantities derived from (6) are also functionals of the bilocal kernel G^{-1} . In particular, we are interested in studying the functional dependence of the partition function, defined by a functional integral over a Boltzmann weight in natural units

$$Z[G^{-1}] = \int \mathcal{D}\phi e^{-E[\phi, G^{-1}]},
 \tag{7}$$

and the (negative) vacuum energy

$$W[G^{-1}] = \ln Z[G^{-1}].
 \tag{8}$$

For the sake of simplicity we restrict ourselves in the present paper to study the disordered, symmetric phase of the ϕ^4 -theory where the n -point functions

$$\mathbf{G}_{1\dots n}[G^{-1}] = \frac{1}{Z[G^{-1}]} \int \mathcal{D}\phi \phi_1 \dots \phi_n e^{-E[\phi, G^{-1}]},
 \tag{9}$$

with odd n vanish. Thus, the first nonvanishing n -point functions are the two-point function

$$\mathbf{G}_{12}[G^{-1}] = \frac{1}{Z[G^{-1}]} \int \mathcal{D}\phi \phi_1 \phi_2 e^{-E[\phi, G^{-1}]}
 \tag{10}$$

and the four-point function

$$\mathbf{G}_{1234}[G^{-1}] = \frac{1}{Z[G^{-1}]} \int \mathcal{D}\phi \phi_1 \phi_2 \phi_3 \phi_4 e^{-E[\phi, G^{-1}]}.
 \tag{11}$$

Further important statistical quantities are the correlation functions, i.e., the connected n -point functions. In the disordered, symmetric phase, the connected two-point function coincides with the two-point function

$$\mathbf{G}_{12}^c[G^{-1}] = \mathbf{G}_{12}[G^{-1}],
 \tag{12}$$

whereas the connected four-point function is defined by

$$\begin{aligned}
 \mathbf{G}_{1234}^c[G^{-1}] &\equiv \mathbf{G}_{1234}[G^{-1}] - \mathbf{G}_{12}[G^{-1}]\mathbf{G}_{34}[G^{-1}] - \mathbf{G}_{13}[G^{-1}]\mathbf{G}_{24}[G^{-1}] \\
 &\quad - \mathbf{G}_{14}[G^{-1}]\mathbf{G}_{23}[G^{-1}].
 \end{aligned}
 \tag{13}$$

By expanding the functional integrals (7) and (9) in powers of the coupling constant g , the expansion coefficients of the partition function and the n -point functions consist

of free-field expectation values. These are evaluated with the help of Wick’s rule as a sum of Feynman integrals, which are pictured as diagrams constructed from lines and vertices. Thereby the free correlation function G_{12} , which is the functional inverse of the kernel G^{-1} in the energy functional (2)

$$\int_2 G_{12} G_{23}^{-1} = \delta_{13} \tag{14}$$

with $\delta_{13} = \delta_{x_1, x_3} \delta(x_1 - x_3)$, is represented by a line in a Feynman diagram

$$G_{12} \equiv 1 \text{ --- } 2 \quad , \tag{15}$$

and the interaction V is pictured as a vertex

$$- V_{1234} \equiv \begin{array}{c} 2 \quad 3 \\ \diagdown \quad / \\ 1 \quad 4 \end{array} \quad . \tag{16}$$

The graphical elements (15) and (16) are combined by an integral which graphically corresponds to the gluing prescription

$$- \int_4 V_{1234} G_{45} \equiv \begin{array}{c} 2 \quad 3 \\ \diagdown \quad / \\ 1 \quad 4 \end{array} \text{ --- } 5 \equiv \begin{array}{c} 2 \quad 3 \\ \diagdown \quad / \\ 1 \quad 5 \end{array} \quad . \tag{17}$$

In this paper we analyze the resulting diagrams for the statistical quantities (7)–(13) by using their functional dependence on the kernel G_{12}^{-1} . To this end we introduce the functional derivative with respect to the kernel G_{12}^{-1} whose basic rule reflects the symmetry of its indices

$$\frac{\delta G_{12}^{-1}}{\delta G_{34}^{-1}} = \frac{1}{2} (\delta_{13} \delta_{42} + \delta_{14} \delta_{32}) \quad . \tag{18}$$

From identity (14) and the functional product rule we find the effect of this derivative on the free correlation function

$$- \frac{\delta G_{12}}{\delta G_{34}^{-1}} = \frac{1}{2} (G_{13} G_{42} + G_{14} G_{32}) \quad , \tag{19}$$

which has the graphical representation

$$- \frac{\delta}{\delta G_{34}^{-1}} 1 \text{ --- } 2 = \frac{1}{2} \left(1 \text{ --- } 3 \quad 4 \text{ --- } 2 + 1 \text{ --- } 4 \quad 3 \text{ --- } 2 \right) \quad . \tag{20}$$

Thus, a functional derivative with respect to the kernel G_{12}^{-1} is represented by a graphical operation which cuts a line of a Feynman diagram in all possible ways [36–42]. For practical purposes it is convenient to use also functional derivatives with respect to the free correlation function G_{12} whose basic rule reads

$$\frac{\delta G_{12}}{\delta G_{34}} \equiv \frac{\delta 1 \text{ --- } 2}{\delta 3 \text{ --- } 4} = \frac{1}{2} (\delta_{13} \delta_{42} + \delta_{14} \delta_{32}) \quad . \tag{21}$$

Such functional derivatives are represented graphically by removing a line of a Feynman diagram in all possible ways [36–42]. The functional derivatives with respect to the kernel G_{12}^{-1} and the correlation function G_{12} are related via the functional chain rule

$$\frac{\delta}{\delta G_{12}^{-1}} = - \int_{34} G_{13} G_{24} \frac{\delta}{\delta G_{34}} . \tag{22}$$

These functional derivatives are used in Section 2.1 to derive a closed set of Schwinger–Dyson equations for the connected two- and four-point functions. In Section 2.2 they are converted into graphical recursion relations for the corresponding connected Feynman diagrams. Finally, the connected vacuum diagrams contributing to the vacuum energy are constructed in a graphical way in Section 2.3.

2.1. Closed set of equations for connected two- and four-point function

In this subsection we apply the functional derivatives introduced so far to a functional identity which immediately follows from the definition of the functional integral. By doing so, we derive a closed set of Schwinger–Dyson equations determining the connected two- and four-point function.

2.1.1. Connected two-point function

In order to derive an equation for the connected two-point function, we start with the trivial identity

$$\int \mathcal{D}\phi \frac{\delta}{\delta \phi_1} (\phi_2 e^{-E[\phi]}) = 0 , \tag{23}$$

which follows via direct functional integration from the vanishing of the exponential at infinite fields. Taking into account the explicit form of the energy functional (2), we perform the functional derivative with respect to the field and obtain

$$\int \mathcal{D}\phi \left(\delta_{12} - \int_3 G_{13}^{-1} \phi_2 \phi_3 - \frac{1}{6} \int_{345} V_{1345} \phi_2 \phi_3 \phi_4 \phi_5 \right) e^{-E[\phi]} = 0 . \tag{24}$$

Applying the definitions (7)–(13), this equation can be expressed in terms of the connected two- and four-point function as follows:

$$\delta_{12} - \int_3 G_{13}^{-1} \mathbf{G}_{23} = \frac{1}{2} \int_{345} V_{1345} \mathbf{G}_{34} \mathbf{G}_{52} + \frac{1}{6} \int_{345} V_{1345} \mathbf{G}_{2345}^c . \tag{25}$$

Multiplying this equation with G_{16} and integrating with respect to the index 1 finally leads to the Schwinger–Dyson equation which determines the connected two-point function

$$\mathbf{G}_{12} = G_{12} - \frac{1}{2} \int_{3456} G_{13} V_{3456} \mathbf{G}_{45} \mathbf{G}_{62} - \frac{1}{6} \int_{3456} G_{13} V_{3456} \mathbf{G}_{2456}^c . \tag{26}$$

When the connected two-point function is graphically represented in terms of Feynman diagrams by a double line

$$G_{12} \equiv \text{1} \text{====} \text{2} \quad , \quad (27)$$

and the connected four-point function is pictured by a vertex with an open dot with four legs

$$G_{1234}^c \equiv \begin{array}{c} 2 \quad 3 \\ \diagdown \quad / \\ \circ \\ / \quad \diagdown \\ 1 \quad 4 \end{array} \quad , \quad (28)$$

this Schwinger–Dyson equation reads graphically

$$\text{1} \text{====} \text{2} = \text{1} \text{---} \text{2} + \frac{1}{2} \text{1} \text{---} \text{1} \text{---} \text{2} + \frac{1}{6} \text{1} \text{---} \text{1} \text{---} \text{1} \text{---} \text{2} \quad . \quad (29)$$

It represents an integral equation for the connected two-point function on the left-hand side which turns out to appear also on the right-hand side. Iteratively solving the integral equation (29) for the connected two-point function G_{12} necessitates, however, the knowledge of the connected four-point function G_{1234}^c .

2.1.2. Connected four-point function

In principle, one could determine the connected four-point function (13) from the connected two-point function (10) as follows. We obtain from (2) and (18)

$$\phi_1 \phi_2 = 2 \frac{\delta E[\phi]}{\delta G_{12}^{-1}} \quad , \quad (30)$$

so that we yield from (7), (11), and (13)

$$G_{1234}^c = -2 \frac{\delta G_{12}}{\delta G_{34}^{-1}} - G_{13} G_{24} - G_{14} G_{23} \quad . \quad (31)$$

This result reads graphically

$$\begin{array}{c} 2 \quad 3 \\ \diagdown \quad / \\ \circ \\ / \quad \diagdown \\ 1 \quad 4 \end{array} = -2 \frac{\delta \text{1} \text{====} \text{2}}{\delta G_{34}^{-1}} - \text{1} \text{====} \text{3} \text{2} \text{====} \text{4} - \text{1} \text{====} \text{4} \text{2} \text{====} \text{3} \quad . \quad (32)$$

However, such a procedure would have the disadvantage that cutting a line in the diagrams of the connected two-point function G_{12} would also lead to disconnected diagrams which are later on removed by the second and the third term on the right-hand side of (32). As the number of undesired disconnected diagrams occurring at an intermediate step of the calculation increases with the loop order, this procedure is quite inefficient to determine the connected four-point function G_{1234}^c . Therefore, we aim at deriving another equation for G_{1234}^c whose iterative solution only involves connected diagrams. To this end we insert the Schwinger–Dyson equation (26) into relation (31)

and obtain

$$\begin{aligned}
 \mathbf{G}_{1234}^c &= \frac{1}{3} \int_{5678} G_{15} V_{5678} \frac{\delta \mathbf{G}_{6782}^c}{\delta G_{34}^{-1}} - \int_{5678} G_{15} V_{5678} \mathbf{G}_{62} \mathbf{G}_{73} \mathbf{G}_{84} \\
 &\quad - \frac{1}{2} \int_{5678} G_{15} V_{5678} \mathbf{G}_{6734}^c \mathbf{G}_{82} - \frac{1}{2} \int_{5678} G_{15} V_{5678} \mathbf{G}_{8234}^c \mathbf{G}_{67} \\
 &\quad + \frac{1}{6} \int_{5678} G_{15} V_{5678} \mathbf{G}_{6784}^c \mathbf{G}_{23} + \frac{1}{6} \int_{5678} G_{15} V_{5678} \mathbf{G}_{6783}^c \mathbf{G}_{24} . \tag{33}
 \end{aligned}$$

The last two terms in (33) are still disconnected and cancel the disconnected diagrams which are generated by the functional derivative of the connected four-point function with respect to the kernel in the first term. In order to eliminate all disconnected terms from (33) we use the commutator relation

$$\begin{aligned}
 \frac{\delta \mathbf{G}_{1234}^c}{\delta G_{56}^{-1}} - \frac{\delta \mathbf{G}_{1256}^c}{\delta G_{34}^{-1}} &= \frac{1}{2} (\mathbf{G}_{13} \mathbf{G}_{2456}^c + \mathbf{G}_{14} \mathbf{G}_{2356}^c + \mathbf{G}_{23} \mathbf{G}_{1456}^c + \mathbf{G}_{24} \mathbf{G}_{1356}^c \\
 &\quad - \mathbf{G}_{15} \mathbf{G}_{2346}^c - \mathbf{G}_{16} \mathbf{G}_{2345}^c - \mathbf{G}_{25} \mathbf{G}_{1346}^c - \mathbf{G}_{26} \mathbf{G}_{1345}^c) , \tag{34}
 \end{aligned}$$

which directly follows from (31) because of the identity that mixed second functional derivatives with respect to the kernel G^{-1} can be interchanged

$$\frac{\delta^2 \mathbf{G}_{12}}{\delta G_{56}^{-1} \delta G_{34}^{-1}} = \frac{\delta^2 \mathbf{G}_{12}}{\delta G_{34}^{-1} \delta G_{56}^{-1}} . \tag{35}$$

The commutator relation (34) states that within the functional derivative of the connected four-point function with respect to the kernel indices might be interchanged at the expense of the additional terms on the right-hand side. Inserting (34) in (33) by taking into account the Schwinger–Dyson equation (26) and the functional chain rule (22), we yield the following functional integrodifferential equation for the connected four-point function:

$$\begin{aligned}
 \mathbf{G}_{1234}^c &= - \int_{5678} G_{15} V_{5678} \mathbf{G}_{62} \mathbf{G}_{73} \mathbf{G}_{84} - \frac{1}{3} \int_{5678} G_{15} V_{5678} G_{69} G_{70} \frac{\delta \mathbf{G}_{8234}^c}{\delta G_{90}} \\
 &\quad - \frac{1}{6} \int_{5678} G_{15} V_{5678} \mathbf{G}_{8234}^c \mathbf{G}_{67} - \frac{1}{6} \int_{5678} G_{15} V_{5678} \mathbf{G}_{6723}^c \mathbf{G}_{84} \\
 &\quad - \frac{1}{6} \int_{5678} G_{15} V_{5678} \mathbf{G}_{6724}^c \mathbf{G}_{83} - \frac{1}{6} \int_{5678} G_{15} V_{5678} \mathbf{G}_{6734}^c \mathbf{G}_{82} . \tag{36}
 \end{aligned}$$

Although Eq. (36) has the disadvantage of being more complex than Eq. (31), it has the advantage that it does not lead to disconnected diagrams at an intermediate stage of the calculation. This can be immediately seen in its graphical representation

which reads

$$\begin{aligned}
 \text{Diagram 1} &= \text{Diagram 2} + \frac{1}{3} \text{Diagram 3} + \frac{1}{6} \text{Diagram 4} + \frac{1}{6} \text{Diagram 5} \\
 &+ \frac{1}{6} \text{Diagram 6} + \frac{1}{6} \text{Diagram 7} + \frac{1}{6} \text{Diagram 8} .
 \end{aligned}
 \tag{37}$$

Thus the closed set of Schwinger–Dyson equations for the connected two- and four-point function is given by (29) and (37).

2.2. Graphical recursion relations

Now we demonstrate how the diagrams of the connected two- and four-point function are recursively generated in a graphical way. To this end we perform for both quantities a perturbative expansion

$$1 \text{---} 2 \equiv \sum_{p=0}^{\infty} 1 \overset{(p)}{\text{---}} 2 , \tag{38}$$

$$\text{Diagram 1} \equiv \sum_{p=0}^{\infty} \text{Diagram 2} , \tag{39}$$

where p denotes the number of interactions V which contribute. With these we obtain from (29) and (37) the following closed set of graphical recursion relations:

$$1 \overset{(p+1)}{\text{---}} 2 = \frac{1}{2} \sum_{q=0}^p 1 \overset{(p-q)}{\text{---}} 2 + \frac{1}{6} \text{Diagram 1} , \tag{40}$$

$$\begin{aligned}
 \text{Diagram 1} &= \sum_{q=0}^p \sum_{r=0}^q \text{Diagram 2} + \frac{1}{3} \text{Diagram 3} + \frac{1}{6} \text{Diagram 4} + \frac{1}{6} \sum_{q=1}^p \text{Diagram 5} \\
 &+ \frac{1}{6} \sum_{q=1}^p \text{Diagram 6} + \frac{1}{6} \sum_{q=1}^p \text{Diagram 7} + \frac{1}{6} \sum_{q=1}^p \text{Diagram 8} .
 \end{aligned}
 \tag{41}$$

This is solved starting from

$$1 \overset{(0)}{\equiv} 2 = 1 \text{ --- } 2, \tag{42}$$

$$\begin{array}{c} 2 \\ \diagdown \\ \textcircled{0} \\ \diagup \\ 3 \\ 1 \quad 4 \end{array} = 0. \tag{43}$$

Note that these graphical recursion relations (40)–(43) allow to prove via complete induction that all diagrams contributing to the connected two- and four-point function are, indeed, connected [44].

The first few perturbative contributions to G_{12} and G_{1234}^c are determined as follows. Inserting (42) and (43) in (40) and (41), we obtain for $p = 1$ the connected two-point function

$$1 \overset{(1)}{\equiv} 2 = \frac{1}{2} 1 \text{ --- } \textcircled{\bullet} \text{ --- } 2 \tag{44}$$

and the connected four-point function

$$\begin{array}{c} 2 \\ \diagdown \\ \textcircled{1} \\ \diagup \\ 3 \\ 1 \quad 4 \end{array} = \begin{array}{c} 2 \\ \diagdown \\ \times \\ \diagup \\ 3 \\ 1 \quad 4 \end{array}. \tag{45}$$

With this we get from (40) the second-order contribution to the connected two-point function

$$1 \overset{(2)}{\equiv} 2 = \frac{1}{4} 1 \text{ --- } \textcircled{\bullet} \text{ --- } \textcircled{\bullet} \text{ --- } 2 + \frac{1}{4} 1 \text{ --- } \textcircled{\bullet} \text{ --- } \textcircled{\bullet} \text{ --- } 2 + \frac{1}{6} 1 \text{ --- } \textcircled{\bullet} \text{ --- } 2. \tag{46}$$

Amputating one line from (45), i.e.,

$$\begin{aligned}
 \frac{\delta}{\delta 6 \text{ --- } 7} \begin{array}{c} 2 \\ \diagdown \\ \textcircled{1} \\ \diagup \\ 3 \\ 5 \quad 4 \end{array} &= \frac{1}{2} \delta_{26} \begin{array}{c} 7 \\ | \\ 5 \text{ --- } 3 \\ | \\ 4 \end{array} + \frac{1}{2} \delta_{36} \begin{array}{c} 2 \\ | \\ 5 \text{ --- } 7 \\ | \\ 4 \end{array} + \frac{1}{2} \delta_{46} \begin{array}{c} 2 \\ | \\ 5 \text{ --- } 3 \\ | \\ 7 \end{array} + \frac{1}{2} \delta_{27} \begin{array}{c} 6 \\ | \\ 5 \text{ --- } 3 \\ | \\ 4 \end{array} \\
 &+ \frac{1}{2} \delta_{37} \begin{array}{c} 2 \\ | \\ 5 \text{ --- } 6 \\ | \\ 4 \end{array} + \frac{1}{2} \delta_{47} \begin{array}{c} 2 \\ | \\ 5 \text{ --- } 3 \\ | \\ 6 \end{array} + \frac{1}{2} \delta_{56} \begin{array}{c} 2 \\ | \\ 7 \text{ --- } 3 \\ | \\ 4 \end{array} + \frac{1}{2} \delta_{57} \begin{array}{c} 2 \\ | \\ 6 \text{ --- } 3 \\ | \\ 4 \end{array}, \tag{47}
 \end{aligned}$$

we find the second-order contribution to the connected four-point function from (41)

$$\begin{aligned}
 \begin{array}{c} 2 \\ \diagup \\ \textcircled{2} \\ \diagdown \\ 1 \end{array} \begin{array}{c} 3 \\ \diagup \\ \textcircled{2} \\ \diagdown \\ 4 \end{array} &= \frac{1}{2} \left(\begin{array}{c} 2 \\ \textcircled{\text{---}} \\ 4 \end{array} \begin{array}{c} 2 \\ \textcircled{\text{---}} \\ 3 \\ | \\ 4 \end{array} + \begin{array}{c} 3 \\ \textcircled{\text{---}} \\ 4 \\ | \\ 1 \end{array} \begin{array}{c} 3 \\ \textcircled{\text{---}} \\ 4 \\ | \\ 1 \end{array} + \begin{array}{c} 4 \\ \textcircled{\text{---}} \\ 1 \\ | \\ 2 \end{array} \begin{array}{c} 4 \\ \textcircled{\text{---}} \\ 1 \\ | \\ 2 \end{array} + \begin{array}{c} 1 \\ \textcircled{\text{---}} \\ 3 \\ | \\ 2 \end{array} \begin{array}{c} 1 \\ \textcircled{\text{---}} \\ 3 \\ | \\ 2 \end{array} \right) \\
 &+ \frac{1}{2} \left(\begin{array}{c} 2 \\ \diagup \\ \textcircled{\text{---}} \\ \diagdown \\ 1 \end{array} \begin{array}{c} 3 \\ \diagup \\ \textcircled{\text{---}} \\ \diagdown \\ 4 \end{array} + \begin{array}{c} 3 \\ \diagup \\ \textcircled{\text{---}} \\ \diagdown \\ 1 \end{array} \begin{array}{c} 4 \\ \diagup \\ \textcircled{\text{---}} \\ \diagdown \\ 2 \end{array} + \begin{array}{c} 4 \\ \diagup \\ \textcircled{\text{---}} \\ \diagdown \\ 1 \end{array} \begin{array}{c} 2 \\ \diagup \\ \textcircled{\text{---}} \\ \diagdown \\ 3 \end{array} \right) . \tag{48}
 \end{aligned}$$

The results (44)–(46), and (48) are listed in Tables 1 and 2 which show all diagrams of the connected two- and four-point function up to the fourth perturbative order irrespective of their spatial indices. However, to evaluate the recursion relations in higher orders, it becomes necessary to reassign the spatial indices to the end points of the diagrams of the connected two- and four-point function in Tables 1 and 2. This involves a decomposition of the weights shown in Tables 1 and 2 due to symmetry considerations. To this end we characterize a diagram by its symmetry degree N . Thus reassigning the spatial indices to the end points of the diagrams of the connected two- and four-point function leads to $24/N$ different diagrams. As an example for determining the symmetry degree N we consider diagram #4.5 in Table 2. Successively assigning the indices 1,2,3,4 to the respective end points leads to $N = 4$:

$$\begin{aligned}
 24 \begin{array}{c} \diagup \\ \textcircled{\text{---}} \\ \diagdown \end{array} &\mapsto 24 \begin{array}{c} \diagup \\ \textcircled{\text{---}} \\ \diagdown \\ 1 \end{array} \mapsto 8 \begin{array}{c} 2 \\ \diagup \\ \textcircled{\text{---}} \\ \diagdown \\ 1 \end{array} + 8 \begin{array}{c} \diagup \\ \textcircled{\text{---}} \\ \diagdown \\ 1 \end{array} + 8 \begin{array}{c} \diagup \\ \textcircled{\text{---}} \\ \diagdown \\ 1 \end{array} \mapsto \\
 &\mapsto 4 \begin{array}{c} 2 \\ \diagup \\ \textcircled{\text{---}} \\ \diagdown \\ 1 \end{array} \begin{array}{c} 3 \\ \diagup \\ \textcircled{\text{---}} \\ \diagdown \\ 4 \end{array} + 4 \begin{array}{c} 2 \\ \diagup \\ \textcircled{\text{---}} \\ \diagdown \\ 1 \end{array} \begin{array}{c} 4 \\ \diagup \\ \textcircled{\text{---}} \\ \diagdown \\ 3 \end{array} + 4 \begin{array}{c} 3 \\ \diagup \\ \textcircled{\text{---}} \\ \diagdown \\ 1 \end{array} \begin{array}{c} 2 \\ \diagup \\ \textcircled{\text{---}} \\ \diagdown \\ 4 \end{array} + 4 \begin{array}{c} 4 \\ \diagup \\ \textcircled{\text{---}} \\ \diagdown \\ 1 \end{array} \begin{array}{c} 2 \\ \diagup \\ \textcircled{\text{---}} \\ \diagdown \\ 3 \end{array} + 4 \begin{array}{c} 3 \\ \diagup \\ \textcircled{\text{---}} \\ \diagdown \\ 1 \end{array} \begin{array}{c} 4 \\ \diagup \\ \textcircled{\text{---}} \\ \diagdown \\ 2 \end{array} + 4 \begin{array}{c} 4 \\ \diagup \\ \textcircled{\text{---}} \\ \diagdown \\ 1 \end{array} \begin{array}{c} 3 \\ \diagup \\ \textcircled{\text{---}} \\ \diagdown \\ 2 \end{array} . \tag{49}
 \end{aligned}$$

Note that the weights of the diagrams of the connected two- and four-point function in Tables 1 and 2 have been determined by solving the graphical recursion relations. However, as a cross-check, they also follow from the formula [25,36,45]

$$w^{(n)} = \frac{n!}{2^{!S+D} 3^{!T} P N} , \tag{50}$$

where n stands for the number of external legs and S, D, T denote the number of self-, double, triple connections between vertices. Furthermore, P stands for the number of vertex permutations leaving the diagrams unchanged.

2.3. Connected vacuum diagrams

The connected vacuum diagrams of ϕ^4 -theory can be generated order by order together with their weights in two ways. In this section we show first that they follow

Table 1
 Diagrams of the connected two-point function and their weights of the ϕ^4 -theory up to four loops characterized by the vector $(S, D, T, P; N)^a$

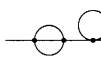
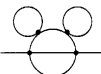
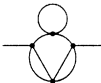
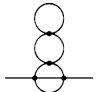
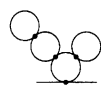
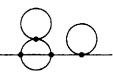
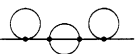
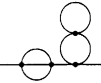
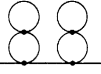
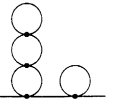
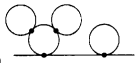
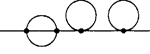
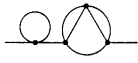
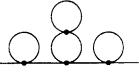
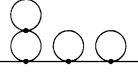
p	<u>(p)</u>			
0	#0.1 1 ——— (0,0,0,1;2)			
1	#1.1 1/2  (1,0,0,1;2)			
2	#2.1 1/6  (0,0,1,1;2)	#2.2 1/4  (1,1,0,1;2)	#2.3 1/4  (2,0,0,1;2)	
3	#3.1 1/4  (0,2,0,1;2)	#3.2 1/12  (0,0,1,2;2)	#3.3 1/4  (1,1,0,1;2)	#3.4 1/8  (1,2,0,1;2)
	#3.5 1/8  (2,0,0,2;2)	#3.6 1/8  (3,0,0,1;2)	#3.7 1/6  (1,0,1,1;1)	#3.8 1/4  (2,1,0,1;1)
4	#4.1 1/8  (0,3,0,1;2)	#4.2 1/4  (0,1,0,2;2)	#4.3 1/4  (0,2,0,1;2)	#4.4 1/12  (0,1,1,1;2)
	#4.5 1/8  (0,2,0,2;2)	#4.6 1/24  (0,1,1,2;2)	#4.7 1/8  (2,1,0,1;2)	#4.8 1/8  (2,0,0,2;2)
	#4.9 1/8  (1,2,0,1;2)	#4.10 1/2  (1,1,0,1;1)	#4.11 1/8  (1,1,0,2;2)	#4.12 1/12  (1,0,1,1;2)
	#4.13 1/8  (1,2,0,1;2)	#4.14 1/16  (2,1,0,2;2)	#4.15 1/8  (2,1,0,1;2)	#4.16 1/16  (3,0,0,2;2)

Table 1 (Continued)

4	#4.17 $\frac{1}{16}$ (1,3,0,1;2)		#4.18 $\frac{1}{36}$ (0,0,2,1;2)		#4.19 $\frac{1}{4}$ (2,1,0,1;1)		#4.20 $\frac{1}{24}$ (2,0,1,1;2)	
	#4.21 $\frac{1}{12}$ (1,0,1,2;1)		#4.22 $\frac{1}{12}$ (1,1,1,1;1)		#4.23 $\frac{1}{16}$ (2,2,0,1;2)		#4.24 $\frac{1}{8}$ (2,2,0,1;1)	
	#4.25 $\frac{1}{8}$ (3,0,0,2;1)		#4.26 $\frac{1}{12}$ (2,0,1,1;1)		#4.27 $\frac{1}{4}$ (1,2,0,1;1)			
	#4.28 $\frac{1}{16}$ (3,1,0,1;2)		#4.29 $\frac{1}{8}$ (3,1,0,1;1)		#4.30 $\frac{1}{16}$ (4,0,0,1;2)			

³Its components S, D, T specify the number of self-, double, triple connections, P stands for the number of vertex permutations leaving the diagram unchanged, and N denotes the symmetry degree of the external legs.

from short-circuiting the external legs of the diagrams of the connected two-point function. Then we elaborate that the connected vacuum diagrams also follow from combining diagrams of the connected two- and four-point function. Thus the latter approach is closely related to Ref. [36], where a nonlinear functional integrodifferential equation for the vacuum energy was recursively solved in a graphical way in order to directly generate the connected vacuum diagrams.

2.3.1. Relation to the diagrams of the connected two-point function

Our first approach is based on the connected two-point function G_{12} . We start with concluding

$$G_{12} = -2 \frac{\delta W}{\delta G_{12}^{-1}}, \tag{51}$$

which follows from (7), (8), and (10) by taking into account (30). We can read off from (51) that cutting a line of the connected diagrams of the vacuum energy in all possible ways leads to all diagrams of the connected two-point function. Here, however, we want to regard (51) as a functional differential equation for the vacuum energy W . If the interaction V vanishes, Eq. (51) is solved by the free contribution of the vacuum energy

$$W^{(0)} = -\frac{1}{2} \text{Tr} \ln G^{-1}. \tag{52}$$

Table 2

Diagrams of the connected four-point function and their weights of the ϕ^4 -theory up to three loops characterized by the vector $(S, D, T, P; N)^a$

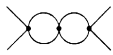
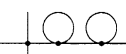
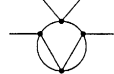
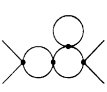
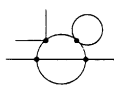
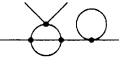
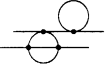
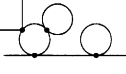
p				
1	#1.1 1 (0,0,0,1;24) 			
2	#2.1 3/2 (0,1,0,1;8) 	#2.2 2 (1,0,0,1;6) 		
3	#3.1 3/4 (0,2,0,1;8) 	#3.2 3 (0,1,0,1;4) 	#3.3 3/2 (1,0,0,1;8) 	#3.4 2/3 (0,0,1,1;6) 
	#3.5 3 (1,1,0,1;2) 	#3.6 3/2 (2,0,0,1;4) 	#3.7 1 (2,0,0,1;6) 	#3.8 1 (1,1,0,1;6) 
4	#4.1 3/8 (0,3,0,1;8) 	#4.2 1 (0,0,0,1;24) 	#4.3 3/2 (0,2,0,1;4) 	#4.4 3/4 (0,1,0,2;8) 
	#4.5 3/2 (0,2,0,1;4) 	#4.6 6 (0,1,0,1;2) 	#4.7 3/2 (0,2,0,1;4) 	#4.8 1/2 (0,0,1,1;8) 
	#4.9 3 (1,0,0,1;4) 	#4.10 3/2 (1,1,0,1;4) 	#4.11 3 (1,1,0,1;2) 	#4.12 3/4 (2,0,0,1;8) 
	#4.13 3/4 (1,1,0,1;8) 	#4.14 3/8 (2,0,0,2;8) 	#4.15 1 (0,2,0,1;6) 	#4.16 1 (0,1,1,1;2) 
	#4.17 3 (1,1,0,1;2) 	#4.18 3 (1,1,0,1;2) 	#4.19 3 (2,0,0,1;2) 	#4.20 3/2 (1,2,0,1;2) 

Table 2 (Continued)

4	<p>#4.21 3/2 (1,2,0,1;2)</p>	<p>#4.22 3/2 (2,1,0,1;2)</p>	<p>#4.23 3/4 (2,1,0,1;4)</p>	<p>#4.24 1 (1,1,0,1;6)</p>
	<p>#4.25 3/2 (2,1,0,1;2)</p>	<p>#4.26 1/2 (2,0,0,2;6)</p>	<p>#4.27 1/2 (3,0,0,1;6)</p>	<p>#4.28 1/3 (0,0,1,2;6)</p>
	<p>#4.29 1/3 (1,0,1,1;6)</p>	<p>#4.30 3/2 (3,0,0,1;2)</p>	<p>#4.31 3/2 (2,1,0,1;2)</p>	
	<p>#4.32 1/2 (2,1,0,1;6)</p>	<p>#4.33 1 (1,0,1,1;2)</p>	<p>#4.34 1/2 (2,1,0,1;6)</p>	
	<p>#4.35 1/3 (1,0,1,1;6)</p>	<p>#4.36 1/2 (3,0,0,1;6)</p>	<p>#4.37 1/2 (1,2,0,1;6)</p>	

^aIts components S, D, T specify the number of self-, double, triple connections, P stands for the number of vertex permutations leaving the diagram unchanged, and N denotes the symmetry degree of the external legs.

Here the trace of the logarithm of the kernel G^{-1} is defined by the series [46, p. 16]

$$\text{Tr} \ln G^{-1} \equiv - \sum_{n=1}^{\infty} \frac{1}{n} \int_{1\dots n} (\delta_{12} - G_{12}^{-1}) \dots (\delta_{n-1,n} - G_{n-1,n}^{-1}) (\delta_{n1} - G_{n1}^{-1}), \quad (53)$$

so that we get

$$-2 \frac{\delta W^{(0)}}{\delta G_{12}^{-1}} = G_{12}. \quad (54)$$

For a nonvanishing interaction V , the functional differential equation (51) produces corrections to (52), which we shall denote with $W^{(int)}$. Thus the vacuum energy decomposes according to

$$W = W^{(0)} + W^{(int)}, \quad (55)$$

and we obtain together with (51) and (54)

$$- \int_{12} G_{12}^{-1} \frac{\delta W^{(int)}}{\delta G_{12}^{-1}} = \frac{1}{2} \int_{12} G_{12}^{-1} (G_{12} - G_{12}). \quad (56)$$

In the following, we aim at recursively determining $W^{(int)}$ in a graphical way. To this end we perform a perturbative expansion of the interaction part of the vacuum energy

$$W^{(int)} = \sum_{p=1}^{\infty} W^{(p)}, \tag{57}$$

and a corresponding one of the connected two-point function

$$G_{12} = G_{12} + \sum_{p=1}^{\infty} G_{12}^{(p)}. \tag{58}$$

Inserting (57) and (58) into (56) and using the functional chain rule (22), we obtain for $p \geq 1$

$$\int_{12} G_{12} \frac{\delta W^{(p)}}{\delta G_{12}} = \frac{1}{2} \int_{12} G_{12}^{-1} G_{12}^{(p)}. \tag{59}$$

The contributions $W^{(p)}$ of the vacuum energy obey the following eigenvalue problem for $p \geq 1$:

$$\int_{12} G_{12} \frac{\delta W^{(p)}}{\delta G_{12}} = 2p W^{(p)}. \tag{60}$$

Indeed, in the p th perturbative order the functional derivative $\delta/\delta G_{12}$ generates diagrams in each of which one of the $2p$ lines of the original vacuum diagram is removed and, subsequently, the removed line is again reinserted. Thus the left-hand side of (60) results in counting the lines of the vacuum diagrams in $W^{(p)}$, so that we obtain the eigenvalue $2p$. With (60) we can explicitly solve (59) for the respective perturbative contributions of the vacuum energy and obtain for $p \geq 1$:

$$W^{(p)} = \frac{1}{4p} \int_{12} G_{12}^{-1} G_{12}^{(p)}. \tag{61}$$

Now we supplement the above-mentioned Feynman rules with a graphical representation for the contributions of the vacuum energy

$$W^{(p)} \equiv \textcircled{p} \tag{62}$$

and for the kernel

$$G_{12}^{-1} \equiv 1 \text{---} \textcircled{\text{---}} \text{---} 2 \tag{63}$$

The latter graphical element serves for gluing two lines together according to

$$\int_{12} G_{31} G_{12}^{-1} G_{24} \equiv 3 \text{---} 1 \text{---} \textcircled{\text{---}} \text{---} 2 \text{---} 4 = 3 \text{---} 4, \tag{64}$$

which follows from

$$\int_{12} G_{31} G_{12}^{-1} G_{24} = G_{34}. \tag{65}$$

Thus our result (61) can be depicted graphically as follows:

$$\textcircled{p} = \frac{1}{4p} \textcircled{\textcircled{p}}. \tag{66}$$

with the respective terms

$$\begin{array}{c} \text{Diagram with 2 vertices and 2 internal lines} \end{array} = \frac{3}{2} \begin{array}{c} \text{Diagram with 3 vertices and 3 internal lines} \end{array} + 2 \begin{array}{c} \text{Diagram with 2 vertices and 1 internal line} \end{array}, \tag{74}$$

$${}^{(0)} \begin{array}{c} \text{Diagram with 2 vertices and 2 internal lines} \end{array} (2) = \frac{1}{6} \begin{array}{c} \text{Diagram with 2 vertices and 1 internal line} \end{array} + \frac{1}{4} \begin{array}{c} \text{Diagram with 4 vertices and 4 internal lines} \end{array} + \frac{1}{4} \begin{array}{c} \text{Diagram with 3 vertices and 3 internal lines} \end{array}, \tag{75}$$

$${}^{(1)} \begin{array}{c} \text{Diagram with 2 vertices and 2 internal lines} \end{array} (1) = \frac{1}{4} \begin{array}{c} \text{Diagram with 4 vertices and 4 internal lines} \end{array}. \tag{76}$$

Thus, we obtain the connected vacuum diagrams shown in Table 3 for $p = 3$:

$$\begin{array}{c} \text{Diagram with 3 vertices and 3 internal lines} \end{array} = \frac{1}{48} \begin{array}{c} \text{Diagram with 3 vertices and 3 internal lines} \end{array} + \frac{1}{24} \begin{array}{c} \text{Diagram with 2 vertices and 1 internal line} \end{array} + \frac{1}{32} \begin{array}{c} \text{Diagram with 4 vertices and 4 internal lines} \end{array} + \frac{1}{48} \begin{array}{c} \text{Diagram with 3 vertices and 3 internal lines} \end{array}. \tag{77}$$

The results (67), (68), and (77) are listed in Table 3 which shows also one further perturbative order. Note that the weights of the connected vacuum diagrams obey a formula similar to (50)

$$w = \frac{1}{2!^{S+D} 3!^T 4!^F P}, \tag{78}$$

where S, D, T, F denote the number of self-, double, triple, fourfold connections and P stands for the number of vertex permutations leaving the vacuum diagram unchanged [25,36,45].

3. One-particle irreducible Feynman diagrams

So far, we have explained how to generate connected Feynman diagrams of the ϕ^4 -theory. We shall now eliminate from them the reducible contributions. To this end we derive in Section 3.1 a closed set of Schwinger–Dyson equations for the one-particle irreducible two- and four-point function. In Section 3.2 they are converted into graphical recursion relations for the corresponding one-particle irreducible Feynman diagrams needed for renormalizing the ϕ^4 -theory. Section 3.3 discusses how these Feynman diagrams of the one-particle irreducible two- and four-point functions are related to the connected vacuum diagrams which are also one-particle irreducible.

3.1. Closed set of Schwinger–Dyson equations for one-particle irreducible two- and four-point functions

In this subsection we revisit the functional identity (25) which immediately followed from the definition of the functional integral. We show that it can be also used to derive a closed set of Schwinger–Dyson equations for the one-particle irreducible two- and four-point functions.

Table 3
Vacuum diagrams and their weights of the ϕ^4 -theory up to five loops^a

p				
1	#1.1 $1/8$ (2,0,0,0,1)			
2	#2.1 $1/48$ (0,0,0,1,2)	#2.2 $1/16$ (2,1,0,0,2)		
3	#3.1 $1/48$ (0,3,0,0,6)	#3.2 $1/24$ (1,0,1,0,2)	#3.3 $1/48$ (3,0,0,0,6)	#3.4 $1/32$ (2,2,0,0,2)
4	#4.1 $1/128$ (0,4,0,0,8)	#4.2 $1/32$ (0,2,0,0,8)	#4.3 $1/144$ (0,0,2,0,4)	#4.4 $1/16$ (1,2,0,0,2)
	#4.5 $1/48$ (2,0,1,0,2)	#4.6 $1/32$ (2,1,0,0,4)	#4.7 $1/48$ (1,1,1,0,2)	#4.8 $1/32$ (3,1,0,0,2)
	#4.9 $1/128$ (4,0,0,0,8)	#4.10 $1/64$ (2,3,0,0,2)		

^aEach diagram is characterized by the vector (S,D,T,F,P) whose components specify the number of self-, double, triple and fourfold connections, and of the vertex permutations leaving the vacuum diagram unchanged, respectively.

3.1.1. Field-theoretic definitions

From Table 1 we can distinguish two classes of diagrams contributing to the connected two-point function G_{12} . The first one contains one-particle irreducible diagrams

which remain connected after amputating one arbitrary line. The second one consists of the remaining diagrams which are called reducible. The diagrams #2.1 and #2.2, for instance, are one-particle irreducible, whereas #2.3 is reducible. When considering the self-energy

$$\Sigma_{12} = G_{12}^{-1} - \mathbf{G}_{12}^{-1}, \tag{79}$$

where \mathbf{G}_{12}^{-1} is the functional inverse of \mathbf{G}_{12} :

$$\int_3 \mathbf{G}_{13} \mathbf{G}_{32}^{-1} \equiv \delta_{12}, \tag{80}$$

we will see later on that this quantity is graphically represented by all one-particle irreducible diagrams of the connected two-point function \mathbf{G}_{12} where the external legs are omitted. Reversely, all connected diagrams of the connected two-point function \mathbf{G}_{12} are reconstructed from the one-particle irreducible ones of the self-energy Σ_{12} according to the Dyson equation

$$\mathbf{G}_{12} = G_{12} + \int_{34} G_{13} \Sigma_{34} \mathbf{G}_{42}, \tag{81}$$

which immediately follows from (79) by taking into account (14) and (80). When the self-energy is graphically represented in Feynman diagrams by a big open dot with two legs

$$\Sigma_{12} \equiv 1 \text{---} \bigcirc \text{---} 2, \tag{82}$$

the Dyson equation (81) reads graphically

$$1 \text{====} 2 = 1 \text{---} 2 + 1 \text{---} \bigcirc \text{====} 2. \tag{83}$$

In a similar way, Table 2 shows that the diagrams of the connected four-point function \mathbf{G}_{1234} are either one-particle irreducible, as for instance diagram #2.1, or reducible such as #2.2. Defining

$$\Gamma_{1234} = - \int_{5678} \mathbf{G}_{5678}^c \mathbf{G}_{51}^{-1} \mathbf{G}_{62}^{-1} \mathbf{G}_{73}^{-1} \mathbf{G}_{84}^{-1}, \tag{84}$$

we will see later on that this quantity consists of all one-particle irreducible diagrams of the connected four-point function \mathbf{G}_{1234} where the external legs are omitted. Therefore, this quantity Γ_{1234} is called the one-particle irreducible four-point function. Inverting relation (84) yields

$$\mathbf{G}_{1234}^c = - \int_{5678} \Gamma_{5678} \mathbf{G}_{51} \mathbf{G}_{62} \mathbf{G}_{73} \mathbf{G}_{84}. \tag{85}$$

When the one-particle four-point function is depicted by using a big open dot with four legs

$$-\Gamma_{1234} \equiv \begin{array}{c} 2 & & 3 \\ & \diagdown & / \\ & \bigcirc & \\ & / & \diagdown \\ 1 & & 4 \end{array}, \tag{86}$$

identity (85) reads graphically

$$\begin{array}{c} 2 \\ \diagup \\ \circ \\ \diagdown \\ 1 \end{array} \begin{array}{c} 3 \\ \diagdown \\ \circ \\ \diagup \\ 4 \end{array} = \begin{array}{c} 2 \\ \diagup \\ \circ \\ \diagdown \\ 1 \end{array} \begin{array}{c} 3 \\ \diagdown \\ \circ \\ \diagup \\ 4 \end{array} . \tag{87}$$

In the following we determine a closed set of Schwinger–Dyson equations for the self-energy and the one-particle irreducible four-point function.

3.1.2. Self-energy

Multiplying identity (25) with G_{27}^{-1} and integrating with respect to the index 2, we take into account self-energy (79) as well as the connected four-point function (85). Thus we yield the Schwinger–Dyson equation for the self-energy

$$\Sigma_{12} = -\frac{1}{2} \int_{34} V_{1234} G_{34} + \frac{1}{6} \int_{345678} V_{1345} G_{36} G_{47} G_{58} \Gamma_{6782} . \tag{88}$$

Its graphical representation reads

$$1 \text{---} \text{---} \text{---} 2 = \frac{1}{2} \text{---} \text{---} \text{---} 2 + \frac{1}{6} \text{---} \text{---} \text{---} 2 . \tag{89}$$

It contains on the right-hand side the connected two-point function which is determined by the Dyson equation (83). Iteratively solving the integral equations (83) and (89) necessitates, however, the knowledge of the one-particle irreducible four-point function Γ_{1234} .

3.1.3. One-particle irreducible four-point function

In principle, one could determine Γ_{1234} from the self-energy Σ_{12} . To this end we insert relation (31) into the definition (84) of the one-particle irreducible four-point function

$$\Gamma_{1234} = 2 \int_{5678} \frac{\delta G_{56}}{\delta G_{78}^{-1}} G_{51}^{-1} G_{62}^{-1} G_{73}^{-1} G_{84}^{-1} + G_{13}^{-1} G_{24}^{-1} + G_{14}^{-1} G_{23}^{-1} . \tag{90}$$

The functional derivative on the right-hand side follows from applying a functional derivative with respect to the kernel G^{-1} to identity (80)

$$\frac{\delta G_{56}}{\delta G_{78}^{-1}} = - \int_{90} G_{59} \frac{\delta G_{90}^{-1}}{\delta G_{78}^{-1}} G_{06} . \tag{91}$$

Using the definition of self-energy (79) and Eq. (18), the one-particle irreducible four-point function (90) reduces to

$$\Gamma_{1234} = 2 \int_{56} G_{35}^{-1} \frac{\delta \Sigma_{12}}{\delta G_{56}^{-1}} G_{64}^{-1} . \tag{92}$$

Applying again (79) and the functional chain rule (22), this yields

$$\begin{aligned} -\Gamma_{1234} = & 2 \frac{\delta \Sigma_{12}}{\delta G_{34}} - 2 \int_{56} \Sigma_{35} G_{56} \frac{\delta \Sigma_{12}}{\delta G_{64}} - 2 \int_{56} \frac{\delta \Sigma_{12}}{\delta G_{35}} G_{56} \Sigma_{64} \\ & + 2 \int_{5678} \Sigma_{35} G_{57} \frac{\delta \Sigma_{12}}{\delta G_{78}} G_{86} \Sigma_{64} , \end{aligned} \tag{93}$$

which is represented graphically as

$$\begin{aligned}
 \begin{array}{c} 2 \\ \diagup \\ \bigcirc \\ \diagdown \\ 1 \quad 4 \end{array} \begin{array}{c} 3 \\ \diagdown \\ \bigcirc \\ \diagup \\ 5 \end{array} &= 2 \frac{\delta \begin{array}{c} 1 \\ \bigcirc \\ 2 \end{array}}{\delta \begin{array}{c} 3 \\ \text{---} \\ 4 \end{array}} + 2 \begin{array}{c} 3 \\ \text{---} \\ \bigcirc \\ \text{---} \\ 5 \end{array} \frac{\delta \begin{array}{c} 1 \\ \bigcirc \\ 2 \end{array}}{\delta \begin{array}{c} 5 \\ \text{---} \\ 6 \end{array}} \begin{array}{c} 6 \\ \text{---} \\ \bigcirc \\ \text{---} \\ 4 \end{array} \\
 - 2 \begin{array}{c} 3 \\ \text{---} \\ \bigcirc \\ \text{---} \\ 5 \end{array} \frac{\delta \begin{array}{c} 1 \\ \bigcirc \\ 2 \end{array}}{\delta \begin{array}{c} 5 \\ \text{---} \\ 4 \end{array}} - 2 \frac{\delta \begin{array}{c} 1 \\ \bigcirc \\ 2 \end{array}}{\delta \begin{array}{c} 3 \\ \text{---} \\ 5 \end{array}} \begin{array}{c} 5 \\ \text{---} \\ \bigcirc \\ \text{---} \\ 4 \end{array} .
 \end{aligned}
 \tag{94}$$

Thus amputating a line from the self-energy Σ_{12} leads to the one-particle irreducible diagrams of Γ_{1234} . However, this procedure has the disadvantage that the first two terms yield reducible diagrams which are later on removed in the last two terms in (94). As the number of undesired one-particle reducible diagrams occurring at an intermediate step of the calculation increases with the loop order, the procedure of determining Γ_{1234} via relation (94) is quite inefficient. Therefore, we aim at deriving another equation for Γ_{1234} whose iterative solution only involves one-particle irreducible diagrams.

Going back to Eq. (92), we insert the Schwinger–Dyson equation (88) for the self-energy and obtain

$$\begin{aligned}
 \Gamma_{1234} &= V_{1234} - \frac{g}{2} \int_{5678} V_{1256} \mathbf{G}_{57} \mathbf{G}_{68} \Gamma_{7834} - \frac{1}{2} \int_{5678} V_{1356} \mathbf{G}_{57} \mathbf{G}_{68} \Gamma_{7824} \\
 &\quad - \frac{1}{2} \int_{5678} V_{1456} \mathbf{G}_{57} \mathbf{G}_{68} \Gamma_{7823} + \frac{1}{2} \int_{567890\bar{1}\bar{2}} V_{5167} \mathbf{G}_{69} \mathbf{G}_{70} \Gamma_{902\bar{1}} \mathbf{G}_{\bar{1}\bar{2}} \Gamma_{\bar{2}348} \mathbf{G}_{85} \\
 &\quad + \frac{1}{3} \int_{567890\bar{1}\bar{2}} V_{1567} \mathbf{G}_{58} \mathbf{G}_{69} \mathbf{G}_{70} \frac{\delta \Gamma_{8902}}{\delta \mathbf{G}_{\bar{1}\bar{2}}^{-1}} \mathbf{G}_{\bar{1}\bar{3}}^{-1} \mathbf{G}_{\bar{2}4}^{-1} .
 \end{aligned}
 \tag{95}$$

The last term is still problematic, as inserting definition (79) of the self-energy would yield again an inefficient equation. This time, however, we can circumvent the inefficiency problem by deriving from (92) the commutator relation

$$\begin{aligned}
 &\int_{78} \frac{\delta \Gamma_{1234}}{\delta \mathbf{G}_{78}^{-1}} \mathbf{G}_{75}^{-1} \mathbf{G}_{86}^{-1} - \int_{78} \frac{\delta \Gamma_{1256}}{\delta \mathbf{G}_{78}^{-1}} \mathbf{G}_{73}^{-1} \mathbf{G}_{84}^{-1} \\
 &= 2 \int_{7890\bar{1}\bar{2}} \mathbf{G}_{57}^{-1} \mathbf{G}_{68}^{-1} \frac{\delta}{\delta \mathbf{G}_{78}^{-1}} (\mathbf{G}_{39}^{-1} \mathbf{G}_{40}^{-1}) \mathbf{G}_{9\bar{1}} \mathbf{G}_{0\bar{2}} \Gamma_{\bar{1}\bar{2}12} \\
 &\quad - 2 \int_{7890\bar{1}\bar{2}} \mathbf{G}_{37}^{-1} \mathbf{G}_{48}^{-1} \frac{\delta}{\delta \mathbf{G}_{78}^{-1}} (\mathbf{G}_{59}^{-1} \mathbf{G}_{60}^{-1}) \mathbf{G}_{9\bar{1}} \mathbf{G}_{0\bar{2}} \Gamma_{\bar{1}\bar{2}12} .
 \end{aligned}
 \tag{96}$$

Applying then

$$\frac{\delta \mathbf{G}_{12}^{-1}}{\delta \mathbf{G}_{34}^{-1}} = \frac{1}{2} (\delta_{13} \delta_{24} + \delta_{14} \delta_{23}) - \frac{1}{2} \int_{56} \mathbf{G}_{35} \Gamma_{5126} \mathbf{G}_{64} ,
 \tag{97}$$

which follows from inserting (92) in (79), the intermediate commutator relation (96) is converted to the final one

$$\begin{aligned} & \int_{78} \frac{\delta \Gamma_{1234}}{\delta G_{78}^{-1}} \mathbf{G}_{75}^{-1} \mathbf{G}_{86}^{-1} - \int_{78} \frac{\delta \Gamma_{1256}}{\delta G_{78}^{-1}} \mathbf{G}_{73}^{-1} \mathbf{G}_{84}^{-1} \\ &= \frac{1}{2} \int_{78} \Gamma_{3457} \mathbf{G}_{78} \Gamma_{8126} + \frac{1}{2} \int_{78} \Gamma_{3467} \mathbf{G}_{78} \Gamma_{8125} \\ & \quad - \frac{1}{2} \int_{78} \Gamma_{5637} \mathbf{G}_{78} \Gamma_{8124} - \frac{1}{2} \int_{78} \Gamma_{5647} \mathbf{G}_{78} \Gamma_{8123} . \end{aligned} \tag{98}$$

Note that the present commutator relation (98) is equivalent to the former one (34) in Section 2. Indeed, Eq. (98) follows also from inserting (85) into (34) after a lengthy but straightforward calculation. Now we can treat the last problematic term in (95) with the commutator relation (98) and thus yield a nonlinear functional integrodifferential equation for the one-particle irreducible four-point function

$$\begin{aligned} -\Gamma_{1234} &= -V_{1234} + \frac{1}{3} \int_{567890} V_{1567} \mathbf{G}_{58} \mathbf{G}_{69} \mathbf{G}_{70} \frac{\delta \Gamma_{8234}}{\delta G_{90}} + \frac{1}{2} \int_{5678} V_{1256} \mathbf{G}_{57} \mathbf{G}_{68} \Gamma_{7834} \\ & \quad + \frac{1}{2} \int_{5678} V_{1356} \mathbf{G}_{57} \mathbf{G}_{68} \Gamma_{7824} + \frac{1}{2} \int_{5678} V_{1456} \mathbf{G}_{57} \mathbf{G}_{68} \Gamma_{7823} \\ & \quad - \frac{1}{6} \int_{567890\bar{1}\bar{2}} V_{5167} \mathbf{G}_{69} \mathbf{G}_{70} \Gamma_{902\bar{1}} \mathbf{G}_{\bar{1}\bar{2}} \Gamma_{\bar{2}348} \mathbf{G}_{85} \\ & \quad - \frac{1}{6} \int_{567890\bar{1}\bar{2}} V_{5167} \mathbf{G}_{69} \mathbf{G}_{70} \Gamma_{903\bar{1}} \mathbf{G}_{\bar{1}\bar{2}} \Gamma_{\bar{2}248} \mathbf{G}_{85} \\ & \quad - \frac{1}{6} \int_{567890\bar{1}\bar{2}} V_{5167} \mathbf{G}_{69} \mathbf{G}_{70} \Gamma_{904\bar{1}} \mathbf{G}_{\bar{1}\bar{2}} \Gamma_{\bar{2}238} \mathbf{G}_{85} . \end{aligned} \tag{99}$$

Its graphical representation reads

$$\begin{aligned} & \text{Diagram 1} = \text{Diagram 2} + \frac{1}{3} \text{Diagram 3} + \frac{1}{2} \text{Diagram 4} + \frac{1}{2} \text{Diagram 5} + \frac{1}{2} \text{Diagram 6} \\ & \quad + \frac{1}{2} \text{Diagram 7} + \frac{1}{6} \text{Diagram 8} + \frac{1}{6} \text{Diagram 9} + \frac{1}{6} \text{Diagram 10} + \frac{1}{6} \text{Diagram 11} . \end{aligned} \tag{100}$$

Thus the closed set of Schwinger–Dyson equations for the connected two-point function, the self-energy and the one-particle irreducible four-point function is given by (83), (89), and (100). In the subsequent section we show that its recursive graphical solution leads to all one-particle irreducible Feynman diagrams needed for renormalizing the ϕ^4 -theory.

3.2. Graphical recursion relations

To this end we supplement the perturbative expansion (38) of the connected two-point function with corresponding ones for the self-energy

$$1 \text{---} \textcircled{p} \text{---} 2 = \sum_{p=1}^{\infty} 1 \text{---} \textcircled{p} \text{---} 2 \tag{101}$$

and for the one-particle irreducible four-point function

$$\begin{matrix} 2 & & 3 \\ & \diagdown & / \\ & \textcircled{p+1} & \\ & / & \diagdown \\ 1 & & 4 \end{matrix} = \sum_{p=1}^{\infty} \begin{matrix} 2 & & 3 \\ & \diagdown & / \\ & \textcircled{p} & \\ & / & \diagdown \\ 1 & & 4 \end{matrix} . \tag{102}$$

As a result we obtain the following closed set of graphical recursion relations:

$$1 \text{---} \textcircled{p} \text{---} 2 = \frac{1}{2} \begin{matrix} (p-1) \\ \textcircled{\textcircled{p-1}} \end{matrix} 2 + \frac{1}{6} \sum_{q=1}^{p-1} \sum_{r=1}^q \sum_{s=1}^r 1 \text{---} \textcircled{\textcircled{\textcircled{p-q-r}}} \text{---} 2 , \tag{103}$$

$$1 \text{---} \textcircled{p} \text{---} 2 = \sum_{q=1}^p 1 \text{---} \textcircled{q} \text{---} \textcircled{p-q} 2 , \tag{104}$$

$$\begin{aligned} \begin{matrix} 2 & & 3 \\ & \diagdown & / \\ & \textcircled{p+1} & \\ & / & \diagdown \\ 1 & & 4 \end{matrix} &= \frac{1}{3} \sum_{q=1}^p 1 \text{---} \textcircled{\textcircled{\textcircled{p-q}}} \text{---} 2 + \frac{1}{2} \sum_{q=1}^p \sum_{r=1}^q \begin{matrix} 2 & & 3 \\ & \diagdown & / \\ & \textcircled{\textcircled{p-q-r}}} & \\ & / & \diagdown \\ 1 & & 4 \end{matrix} + \frac{1}{2} \sum_{q=1}^p \sum_{r=1}^q \begin{matrix} 4 & & 3 \\ & \diagdown & / \\ & \textcircled{\textcircled{p-q-r}}} & \\ & / & \diagdown \\ 1 & & 2 \end{matrix} \\ &+ \frac{1}{2} \sum_{q=1}^p \sum_{r=1}^q \begin{matrix} 3 & & 4 \\ & \diagdown & / \\ & \textcircled{\textcircled{p-q-r}}} & \\ & / & \diagdown \\ 1 & & 2 \end{matrix} + \frac{1}{6} \sum_{q=2}^p \sum_{r=2}^q \sum_{s=2}^r \sum_{t=1}^{s-1} \sum_{k=0}^{t-1} (q-r) \begin{matrix} 2 & & 3 \\ & \diagdown & / \\ & \textcircled{\textcircled{\textcircled{p-q-r}}} & \\ & / & \diagdown \\ 1 & & 4 \end{matrix} \\ &+ \frac{1}{6} \sum_{q=2}^p \sum_{r=2}^q \sum_{s=2}^r \sum_{t=1}^{s-1} \sum_{k=0}^{t-1} (q-r) \begin{matrix} 4 & & 3 \\ & \diagdown & / \\ & \textcircled{\textcircled{\textcircled{p-q-r}}} & \\ & / & \diagdown \\ 1 & & 2 \end{matrix} + \frac{1}{6} \sum_{q=2}^p \sum_{r=2}^q \sum_{s=2}^r \sum_{t=1}^{s-1} \sum_{k=0}^{t-1} (q-r) \begin{matrix} 3 & & 4 \\ & \diagdown & / \\ & \textcircled{\textcircled{\textcircled{p-q-r}}} & \\ & / & \diagdown \\ 1 & & 2 \end{matrix} . \tag{105} \end{aligned}$$

This is to be solved starting from

$$1 \text{---} \textcircled{0} \text{---} 2 = 1 \text{---} 2 , \tag{106}$$

$$\begin{matrix} 2 & & 3 \\ & \diagdown & / \\ & \textcircled{1} & \\ & / & \diagdown \\ 1 & & 4 \end{matrix} = \begin{matrix} 2 & & 3 \\ & \diagdown & / \\ & \times & \\ & / & \diagdown \\ 1 & & 4 \end{matrix} . \tag{107}$$

Note that these graphical recursion relations (103)–(107) allow to prove via complete induction that all diagrams which contribute to the self-energy and the one-particle irreducible four-point function are, indeed, one-particle irreducible [44].

The first few perturbative contributions to Σ_{12} and Γ_{1234} are determined as follows. Inserting (106) in (103) and (104) yield for $p = 1$ the self-energy

$$1 \text{---} \textcircled{1} \text{---} 2 = \frac{1}{2} 1 \text{---} \textcirclearrowright \text{---} 2 \quad , \quad (108)$$

and the connected two-point function

$$1 \text{---} \textcircled{1}^{(1)} \text{---} 2 = 1 \text{---} \textcircled{1}^{(0)} \text{---} 2 = \frac{1}{2} 1 \text{---} \textcirclearrowright \text{---} 2 \quad . \quad (109)$$

As (107) represent a bare vertex with no line, we read off

$$\frac{\delta}{\delta 6 \text{---} 7} \textcircled{1}^{(0)} = 0 \quad . \quad (110)$$

the second-order contribution to the one-particle irreducible four-point function follows from (105) to be

$$\textcircled{2} = \frac{1}{2} \textcirclearrowright + \frac{1}{2} \textcirclearrowleft + \frac{1}{2} \textcirclearrowright \quad . \quad (111)$$

The results in (108), (109), and (111) are then used to determine for $p = 2$ the self-energy (103)

$$1 \text{---} \textcircled{2} \text{---} 2 = \frac{1}{4} 1 \text{---} \textcirclearrowright \text{---} 2 + \frac{1}{6} 1 \text{---} \textcirclearrowright \text{---} 2 \quad (112)$$

and the connected two-point function (104)

$$1 \text{---} \textcircled{2}^{(2)} \text{---} 2 = 1 \text{---} \textcircled{2}^{(0)} \text{---} 2 + 1 \text{---} \textcircled{1}^{(1)} \text{---} 2 = \frac{1}{4} 1 \text{---} \textcirclearrowright \text{---} 2 + \frac{1}{4} 1 \text{---} \textcirclearrowright \text{---} 2 + \frac{1}{6} 1 \text{---} \textcirclearrowright \text{---} 2 \quad . \quad (113)$$

Amputating one line from (111),

$$\begin{aligned} \frac{\delta}{\delta 6 \text{---} 7} \textcircled{2} &= \frac{1}{2} \frac{\delta}{\delta 6 \text{---} 7} \left(\textcirclearrowright + \textcirclearrowleft + \textcirclearrowright \right) \\ &= \frac{1}{2} \left(5 \text{---} \textcirclearrowright \text{---} 4 + 5 \text{---} \textcirclearrowleft \text{---} 4 + 5 \text{---} \textcirclearrowright \text{---} 3 + 5 \text{---} \textcirclearrowleft \text{---} 3 + 5 \text{---} \textcirclearrowright \text{---} 2 + 5 \text{---} \textcirclearrowleft \text{---} 2 \right) \quad , \end{aligned} \quad (114)$$

we find the third-order contribution to the one-particle irreducible four-point function from (105)

$$\begin{aligned}
 & \text{Diagram with a circle containing '3' and four external legs labeled 1, 2, 3, 4} = \frac{1}{4} \left(\text{Diagram 1} + \text{Diagram 2} + \text{Diagram 3} \right) \\
 & + \frac{1}{2} \left(\text{Diagram 4} + \text{Diagram 5} + \text{Diagram 6} + \text{Diagram 7} + \text{Diagram 8} + \text{Diagram 9} \right) \\
 & + \frac{1}{2} \left(\text{Diagram 10} + \text{Diagram 11} + \text{Diagram 12} \right) .
 \end{aligned}
 \tag{115}$$

As expected, diagrams (109) and (113) for the connected two-point function coincide with the ones from Section 2.2 which are shown in Table 1. Furthermore, diagrams (108), (112) and (107), (111), (115) for the self-energy and the one-particle irreducible four-point function are listed in Tables 4 and 5 which show all one-particle irreducible diagrams up to the order $p = 4$ irrespective of their spatial indices (compare the discussion before Eq. (49)). Note that these one-particle irreducible Feynman diagrams have to be evaluated in order to determine the critical exponents of the ϕ^4 -theory from renormalizing the field ϕ , the coupling constant g and the mass m^2 . So far, the results are available up to six and partly to seven loops in $d = 3$ [47–49] and up to five loops in $d = 4 - \epsilon$ dimensions within the minimal subtraction scheme [25,50].

3.3. One-particle irreducible vacuum diagrams

The vacuum diagrams of ϕ^4 -theory are not only connected but also one-particle irreducible. In this section we elaborate how they can be generated from short-circuiting the external legs of the diagrams of the self-energy and the one-particle irreducible four-point function, respectively.

3.3.1. Relation to the diagrams of the self-energy

At first, we consider the approach which is based on the self-energy. Combining the Dyson equation (81) with the perturbative expansion of the connected two-point function (58) and the corresponding one for the self-energy

$$\Sigma_{12} = \sum_{p=1}^{\infty} \Sigma_{12}^{(p)} ,
 \tag{116}$$

we obtain

$$\int_{12} G_{12}^{(p)} G_{12}^{-1} = \sum_{q=1}^p \int_{12} \Sigma_{12}^{(q)} G_{12}^{(p-q)} .
 \tag{117}$$

Table 4

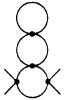
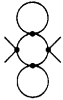
One-particle irreducible diagrams of the self-energy and their weights of the ϕ^4 -theory up to four loops characterized by the vector $(S, D, T, P; N)^a$

p					
1	#1.1 $\frac{1}{2}$ (1,0,0,1;2)				
2	#2.1 $\frac{1}{6}$ (0,0,1,1;2)		#2.2 $\frac{1}{4}$ (1,1,0,1;2)		
3	#3.1 $\frac{1}{4}$ (0,2,0,1;2)	#3.2 $\frac{1}{12}$ (0,0,1,2;2)	#3.3 $\frac{1}{4}$ (1,1,0,1;2)	#3.4 $\frac{1}{8}$ (1,2,0,1;2)	#3.5 $\frac{1}{8}$ (2,0,0,2;2)
	#4.1 $\frac{1}{8}$ (0,3,0,1;2)	#4.2 $\frac{1}{4}$ (0,1,0,2;2)	#4.3 $\frac{1}{4}$ (0,2,0,1;2)	#4.4 $\frac{1}{12}$ (0,1,1,1;2)	#4.5 $\frac{1}{8}$ (0,2,0,2;2)
	#4.6 $\frac{1}{24}$ (0,1,1,2;2)	#4.7 $\frac{1}{8}$ (2,1,0,1;2)	#4.8 $\frac{1}{8}$ (2,0,0,2;2)	#4.9 $\frac{1}{8}$ (1,2,0,1;2)	
	#4.10 $\frac{1}{2}$ (1,1,0,1;1)	#4.11 $\frac{1}{8}$ (1,1,0,2;2)	#4.12 $\frac{1}{12}$ (1,0,1,1;2)	#4.13 $\frac{1}{8}$ (1,2,0,1;2)	
	14 $\frac{1}{16}$ (2,1,0,2;2)	#4.15 $\frac{1}{8}$ (2,1,0,1;2)	#4.16 $\frac{1}{16}$ (3,0,0,2;2)	#4.17 $\frac{1}{16}$ (1,3,0,1;2)	

^aIts components S, D, T specify the number of self-, double, triple connections, P stands for the number of vertex permutations leaving the diagram unchanged, and N denotes the symmetry degree of the external legs.

Table 5

Diagrams of the one-particle four-point function and their weights of the ϕ^4 -theory up to four loops characterized by the vector $(S, D, T, P; N)^a$

p				
1	#1.1 1  $(0,0,0,1;24)$			
2	#2.1 $\frac{3}{2}$  $(0,1,0,1;8)$			
3	#3.1 $\frac{3}{4}$  $(0,2,0,1;8)$	#3.2 3  $(0,1,0,1;4)$	#3.3 $\frac{3}{2}$  $(1,0,0,1;8)$	
4	#4.1 $\frac{3}{8}$  $(0,3,0,1;8)$	#4.2 1  $(0,0,0,1;24)$	#4.3 $\frac{3}{2}$  $(0,2,0,1;4)$	#4.4 $\frac{3}{4}$  $(0,1,0,2;8)$
	#4.5 $\frac{3}{2}$  $(0,2,0,1;4)$	#4.6 6  $(0,1,0,1;2)$	#4.7 $\frac{3}{2}$  $(0,2,0,1;4)$	#4.8 $\frac{1}{2}$  $(0,0,1,1;8)$
	#4.9 3  $(1,0,0,1;4)$	#4.10 $\frac{3}{2}$  $(1,1,0,1;4)$	#4.11 3  $(1,1,0,1;2)$	#4.12 $\frac{3}{4}$  $(2,0,0,1;8)$
	#4.13 $\frac{3}{4}$  $(1,1,0,1;8)$	#4.14 $\frac{3}{8}$  $(2,0,0,2;8)$		

^aIts components S, D, T specify the number of self-, double, triple connections, P stands for the number of vertex permutations leaving the diagram unchanged, and N denotes the symmetry degree of the external legs.

Thus our previous Eq. (61) for determining the contributions of the vacuum energy $W^{(p)}$ from the connected two-point function is converted to

$$W^{(p)} = \frac{1}{4p} \sum_{q=1}^p \int_{12} \Sigma_{12}^{(q)} G_{12}^{(p-q)}. \tag{118}$$

This result reads graphically

$$\textcircled{p} = \frac{1}{4p} \sum_{q=1}^p \textcircled{q} \textcircled{(p-q)} \quad (119)$$

We consider one example how the diagrams of the self-energy lead to the corresponding diagrams of the vacuum energy. For $p = 3$ Eq. (119) reduces to

$$\textcircled{3} = \frac{1}{12} \textcircled{1} \textcircled{(2)} + \frac{1}{12} \textcircled{2} \textcircled{(1)} + \frac{1}{12} \textcircled{3} \textcircled{(0)} \quad (120)$$

with the respective terms

$$\textcircled{1} \textcircled{(2)} = \frac{1}{12} \textcircled{1} \textcircled{2} + \frac{1}{8} \textcircled{1} \textcircled{1} \textcircled{1} + \frac{1}{8} \textcircled{1} \textcircled{1} \textcircled{1} \quad (121)$$

$$\textcircled{2} \textcircled{(1)} = \frac{1}{12} \textcircled{2} \textcircled{1} + \frac{1}{8} \textcircled{1} \textcircled{1} \textcircled{1} \quad (122)$$

$$\textcircled{3} \textcircled{(0)} = \frac{1}{4} \textcircled{3} + \frac{1}{3} \textcircled{1} \textcircled{1} \textcircled{1} + \frac{1}{8} \textcircled{1} \textcircled{1} \textcircled{1} \textcircled{1} + \frac{1}{8} \textcircled{1} \textcircled{1} \textcircled{1} \quad (123)$$

Thus we reobtain the connected vacuum diagrams (77) shown in Table 3 for $p = 3$.

3.3.2. Relation to the diagrams of the one-particle irreducible four-point function

For the sake of completeness we also mention that the vacuum diagrams can be generated from closing the diagrams of the one-particle irreducible four-point function. To this end we insert in Eq. (119) determining the contributions of the vacuum energy the recursion relation (103) for the self-energy and yield

$$\textcircled{p+1} = \frac{1}{8(p+1)} \sum_{q=0}^p \textcircled{q} \textcircled{(p-q)} + \frac{1}{24(p+1)} \sum_{q=1}^p \sum_{r=1}^q \sum_{s=1}^r \sum_{t=1}^s \textcircled{q-r} \textcircled{r-s} \textcircled{s-t} \textcircled{t} \textcircled{(p-q)} \quad (124)$$

Note that this equation follows also directly from the previous recursion relation (72) by taking into account the identity (87) and the perturbative expansions (38), (102).

4. Summary and outlook

In this paper we have derived a closed set of Schwinger–Dyson equations in the disordered, symmetric phase of the ϕ^4 -theory. In particular, we supplemented the well-known integral equations (29) and (89) for the connected two-point function and the self-energy by the new functional integrodifferential equations (37) and (100) for the connected and one-particle irreducible four-point function. Their conversion to graphical recursion relations has allowed us to systematically generate the corresponding connected and one-particle irreducible Feynman diagrams. Furthermore, we have discussed how the short-circuiting of their external legs leads to the associated connected vacuum diagrams. In the subsequent paper [51] we shall elaborate how tadpoles and, more generally, corrections to the connected two-point function as well as the vertex can be successively eliminated by introducing higher Legendre transformations [32–34]. This will lead to graphical recursion relations for the skeleton Feynman diagrams in ϕ^4 -theory.

The recursive graphical solution of our closed set of Schwinger–Dyson equations in ϕ^4 -theory is straightforward and has been carried out in this paper up to the fourth perturbative order by hand. Our iterative procedure can easily be automatized by computer algebra. In Ref. [36] it was demonstrated that the basic graphical operations as amputating a line or gluing two lines together can be formulated with the help of a unique matrix notation for Feynman diagrams. It would be interesting to compare the efficiency of our Schwinger–Dyson approach of generating Feynman diagrams of n -point functions together with their weights with already existing computer programs such as FEYNARTS [4,5], QGRAF [6], or DIANA [7].

We believe that our closed set of Schwinger–Dyson equations for the connected and one-particle irreducible two- and four-point function will turn out to be useful for developing nonperturbative approximations. This may proceed, for instance, as in Ref. [52] which proposes a self-consistent solution of the Dyson equation in ϕ^4 -theory by using a scaling ansatz for the connected two-point function near the phase transition. A similar consideration in Ginzburg–Landau theory has allowed Ref. [53] to analyze the influence of the thermal fluctuations of the order parameter and the vector potential on the superconducting phase transition. A self-consistent solution of our closed Schwinger–Dyson equation may be found via a phenomenological ansatz for the connected and one-particle irreducible two- and four-point function, respectively. Within such an ansatz one has to find how the functional derivative with respect to the free correlation function is approximated, as this operation is crucial in the new Schwinger–Dyson equations (37) and (100).

Acknowledgements

We thank Hagen Kleinert for stimulating discussions and for reading the manuscript.

References

- [1] D. Perret-Gallix, *Int. J. Mod. Phys. C* 6 (1995) 531.
- [2] R. Harlander, M. Steinhauser, *Prog. Part. Nucl. Phys.* 43 (1999) 167.
- [3] T. Hahn, *Nucl. Phys. B* 89 (2000) 231.
- [4] J. Külbeck, M. Böhm, A. Denner, *Comp. Phys. Commun.* 60 (1990) 165.
- [5] T. Hahn, *Comp. Phys. Commun.* 140 (2001) 165.
- [6] P. Nogueira, *J. Comput. Phys.* 105 (1993) 279.
- [7] M. Tentyukov, J. Fleischer, *Comp. Phys. Commun.* 132 (2000) 124.
- [8] B.R. Heap, *J. Math. Phys.* 7 (1966) 1582.
- [9] J.F. Nagle, *J. Math. Phys.* 7 (1966) 1588.
- [10] S. Schelstraete, H. Verschelde, *Z. Phys. C* 67 (1995) 343.
- [11] K. Kajantie, M. Laine, Y. Schröder, *Phys. Rev. D* 65 (2002) 045008.
- [12] J. Schwinger, *Particles, Sources, and Fields*, Vols. I and II, Addison-Wesley, New York, 1973.
- [13] A.A. Abrikosov, L.P. Gorkov, I.E. Dzyaloshinski, *Methods of Quantum Field Theory in Statistical Physics*, Prentice-Hall, Englewood Cliffs, NJ, 1963.
- [14] K. Huang, *Statistical Mechanics*, Wiley, New York, 1963.
- [15] J.D. Bjorken, S.D. Drell, Vol. I: *Relativistic Quantum Mechanics*, Vol. II: *Relativistic Quantum Fields*, McGraw-Hill, New York, 1965.
- [16] A.L. Fetter, J.D. Walecka, *Quantum Theory of Many-Particle Systems*, McGraw-Hill, New York, 1971.
- [17] D.J. Amit, *Field Theory, the Renormalization Group and Critical Phenomena*, McGraw-Hill, New York, 1978.
- [18] C. Itzykson, J.-B. Zuber, *Quantum Field Theory*, McGraw-Hill, New York, 1985.
- [19] J.W. Negele, H. Orland, *Quantum Many-Particle Systems*, Addison-Wesley, New York, 1988.
- [20] M. Le Bellac, *Quantum and Statistical Field Theory*, Oxford Science Publications, Oxford, 1991.
- [21] E.K.U. Gross, E. Runge, O. Heinonen, *Many Particle Theory*, Adam Hilger, Bristol, 1991.
- [22] M.E. Peskin, D.V. Schroeder, *Introduction to Quantum Field Theory*, Addison-Wesley, New York, 1995.
- [23] J. Zinn-Justin, *Quantum Field Theory and Critical Phenomena*, 3rd Edition, Oxford Science Publications, Oxford, 1996.
- [24] G.D. Mahan, *Many-Particle Physics*, 3rd Edition, Kluwer Academic, New York, 2000.
- [25] H. Kleinert, V. Schulte-Frohlinde, *Critical Properties of ϕ^4 -Theories*, World Scientific, Singapore, 2001.
- [26] P.C. Martin, J. Schwinger, *Theory of many-particle systems*, *Phys. Rev.* 115 (1959) 1342.
- [27] L.P. Kadanoff, G. Baym, *Quantum Statistical Mechanics—Green's Function Methods in Equilibrium and Nonequilibrium Problems*, W.A. Benjamin, New York, 1962.
- [28] G. Baym, L.P. Kadanoff, *Phys. Rev.* 124 (1961) 287.
- [29] G. Baym, *Phys. Rev.* 127 (1962) 1391.
- [30] C. De Dominicis, P.C. Martin, *J. Math. Phys.* 5 (1964) 14.
- [31] C. De Dominicis, P.C. Martin, *J. Math. Phys.* 5 (1964) 31.
- [32] A.N. Vasiliev, *Functional Methods in Quantum Field Theory and Statistical Physics*, Gordon and Breach, New York, 1998 (translation from the Russian edition, St. Petersburg University Press, St. Petersburg, 1976).
- [33] H. Kleinert, *Fortschr. Phys.* 30 (1982) 187.
- [34] H. Kleinert, *Fortschr. Phys.* 30 (1982) 351.
- [35] R.F. Streater, A.S. Wightman, *PCT, Spin and Statistics, and All That*, W.A. Benjamin, New York, 1964.
- [36] H. Kleinert, A. Pelster, B. Kastening, M. Bachmann, *Phys. Rev. E* 62 (2000) 1537.
- [37] B. Kastening, *Phys. Rev. E* 61 (2000) 3501.
- [38] A. Pelster, H. Kleinert, *Physica A* 323 (2003) 370.
- [39] H. Kleinert, A. Pelster, B. Van den Bossche, *Physica A* 312 (2002) 141.
- [40] M. Bachmann, H. Kleinert, A. Pelster, *Phys. Rev. D* 61 (2000) 085017.
- [41] A. Pelster, K. Glaum, *Phys. Stat. Sol. B* 237 (2003) 72.
- [42] A. Pelster, H. Kleinert, M. Bachmann, *Ann. Phys. (NY)* 297 (2002) 363.
- [43] A. Pelster, K. Glaum, Recursive graphical construction of tadpole-free Feynman diagrams and their weights in ϕ^4 -theory, in: W. Janke, A. Pelster, H.-J. Schmidt, M. Bachmann (Eds.), *Fluctuating Paths*

and Fields—Dedicated to Hagen Kleinert on the Occasion of His 60th Birthday, World Scientific, Singapore, 2001, p. 269; eprint: [hep-th/0105193](http://arxiv.org/abs/hep-th/0105193).

[44] K. Glaum, M.S. Thesis, FU-Berlin, 2001 (in German).

[45] J. Neu, M.S. Thesis, FU-Berlin, 1990 (in German).

[46] H. Kleinert, Gauge Fields in Condensed Matter, Vol. I, Superflow and Vortex Lines, World Scientific, Singapore, 1989.

[47] B.G. Nickel, D.I. Meiron, G.B. Baker Jr., University of Guelph, preprint (1977), http://www.physik.fu-berlin.de/~kleinert/kleiner_reb8/programs/programs.html.

[48] S.A. Antonenko, A.I. Sokolov, Phys. Rev. E 51 (1995) 1894.

[49] D.B. Murray, B.G. Nickel, University of Guelph, preprint, 1998.

[50] H. Kleinert, J. Neu, V. Schulte-Frohlinde, K.G. Chetyrkin, S.A. Larin, Phys. Lett. B 272 (1991) 39; H. Kleinert, J. Neu, V. Schulte-Frohlinde, K.G. Chetyrkin, S.A. Larin, Phys. Lett. B 319 (1993) 545(E).

[51] A. Pelster, K. Glaum, H. Kleinert, to be published.

[52] A.J. Bray, Phys. Rev. Lett. 32 (1974) 1413.

[53] L. Radzikovsky, Europhys. Lett. 29 (1995) 227.